Proceedings of the 27th National and 5th International ISHMT-ASTFE Heat and Mass Transfer Conference
December 14-17, 2023, IIT Patna, Patna-801106, Bihar, India
IHMTC-2023–279

Experimental Investigation of Stratified Sensible Thermal Energy Storage Using Silicone Oil

Anas A.E Ahmed[1], Rudrodip Majumdar[2], and Sandip K. Saha[1]

[1]Department of Mechanical Engineering, Indian Institute of Technology Bombay, Mumbai-400076, India
[2]EECP, School of Natural Sciences and Engineering, National Institute of Advanced Studies, Bengaluru 560012, India

ABSTRACT

This study experimentally investigates the scarcely studied stratified, oil-based sensible thermal energy storage (STES) tank, to examine the heat retention capability of Hytherm-600 silicone oil during the stand-alone period and its heat dispatchability during the discharging process. To conduct an experimental study on the thermic oil, a vertical cylindrical tank with a helical discharging coil fitted inside is used. Three different oil charging temperatures (50, 70, and 90 °C), and three different discharging flow rates (water) through the helical coil (0.5, 1.25, and 2 L/min) have been considered. The thermal stratification phenomena in oil and the evolution of thermocline have been investigated. Results indicate the formation of a thermocline zone of 154 mm thickness in the lower portion of the tank within 3 h from the commencement of the stand-alone period. The discharging operation fluctuates the thermocline stability in the storage medium (i.e., commercial thermic oil Hytherm-600). During the discharging operation, a water flow rate of 0.5 L/min through the helical coil led to higher discharging efficiencies owing to better heat transfer attributable to the higher water residence time inside the coil. For the aforesaid water flow rate, the average discharging efficiencies are 85.6%, 75.6%, and 81.6% for the charging temperatures of 50, 70, and 90 °C, respectively. Finally, the primary thermocline thickness is found to be constant at 82 mm following the splitting of the initial thermocline during the discharging operation.

Keywords: Sensible heat storage, Stratified tank, Thermocline

1. INTRODUCTION

Sensible thermal energy storage (STES) is inexpensive and easy to operate and maintain. Consequently, these storages find use in a wide array of applications. The efficacy of STES depends on the thermophysical properties of the storage medium, such as diffusivity, thermal conductivity, stability, and material compatibility. Among the various sensible thermal energy storages, the stratified sensible thermal energy storage (SSTES) system has attracted ample attention from researchers over the past few decades since it enhances the energy harnessing features of a TES tank and is significantly less expensive as compared to a two-tank system [1-3]. Immersed discharging coils have been proven to be effective energy-harnessing components for the stratified TES systems deployed catering to low-temperature applications (e.g., domestic hot water (DHW) requirements) [4,5]. The heat transfer coefficients and surface area-to-volume ratios are relatively higher for the curved tubes, leading to enhanced heat transfer.

2. LITERATURE REVIEW AND OBJECTIVE

Generally, water is used as the energy storage medium in low-temperature (up to 90 °C) TES systems, so that the TES can be seamlessly integrated into systems such as solar-heated DHW networks, solar cooling systems, district solar heating systems, or even low-temperature industrial processes. The experimental study by Prabhanjan et al. indicated that the average heat transfer coefficient of the helical coil is greater than that of the straight tube heat exchanger [6]. Numerical investigation on different geometrical configurations of heat exchangers, i.e., helical, conical, and inverted conical coil, for four different flow rates of the working fluid at the coil side, indicated that an inverted conical coil gives a higher temperature of the working fluid at the coil outlet and better thermodynamic quality of the extracted energy than other options [5]. Several correlations have been developed to obtain the inner and outer convection heat transfer coefficients for a helical coil heat exchanger [7]. Moreover, the heat transfer correlations in terms of *Nu*, *Ra,* and *Pr* have been developed by Ayuob et al. [8].

The foregoing discussion indicates that the previously reported works are mostly focused on water-based STES for storage-aided low-temperature applications. Water is preferred as the working fluid due to its high specific heat capacity (4.2 kJ/kg. K) and abundance. However, at ambient pressure, the working temperature of water-based storage systems needs to be maintained below 90 °C for hassle-free single-phase operation, thereby limiting the potential application. As a starting point for exploring the alternate options, this study utilizes Hytherm-600 (silicone oil), a thermic fluid prepared by Hindustan Petroleum Corporation Limited, India. It can provide reliable performance in closed fluid heat transfer systems, with the operating temperature reaching up to 220 °C [9]. Experiments have been conducted systematically to understand the heat retention capability, thermocline evolution, and energy extraction features of the oil-based storage tank. This study facilitates an understanding of the effect of the thermos-physical properties of Hytherm-600 on heat retention during stand-alone operation.

3. EXPERIMENTAL FACILITY AND METHODOLOGY

3.1 Experimental setup

The key components of the experimental setup are shown in **Figure 1**. The experimental setup is built around the storage tank with height, inner, and outer diameters of 654 mm, 163 mm, and 169 mm, respectively. The helical coil height, tube inner diameter, and outer diameter are 292.5 mm, 8 mm, and 9 mm, respectively. The coil is fitted with a spatial clearance of 40 mm from the tank top. The TES, the heating tank, and the pipes are covered with a glass wool insulation of 40 mm thickness, and a thin Al-sheet is wrapped around the glass wool cover to curtail the heat losses. K-type thermocouples are used to capture the temperature readings at various points of the experimental setup.

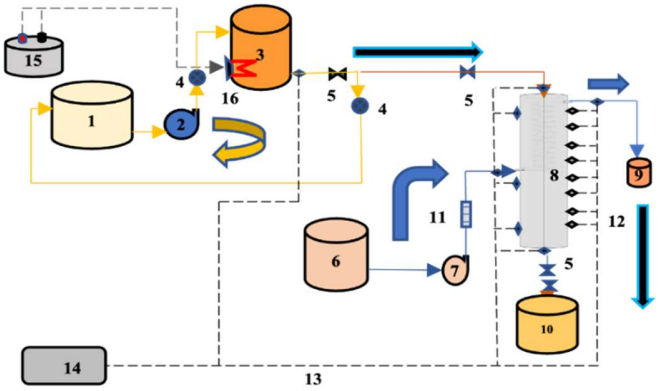

1. Hytherm reservoir tank, 2. Oil pump, 3. Heating tank, 4. Control valves, 5. Needle valves, 6. Cold water reservoir, 7. Centrifugal pump, 8. TES tank with helical coil fitted inside, 9. Water sump tank, 10. Hytherm sump tank, 11. Rotameter, 12. Eight thermocouples fitted inside the TES, 13. Thermocouples wires, 14. Data logger, 15. Variable transformer, 16. Immersion electric heater.

Figure 1: Schematic diagram of the setup

With a penetration depth of 70 mm inside TES, eight thermocouples (*T1* to *T8*) are placed along the height of the TES tank. The successive thermocouples are separated by an axial distance of 82 mm axially. The orientation of the thermocouples is such that there is a 90° angular separation between the successive thermocouples. Such a positioning strategy enables uniform distribution of the thermocouples over the tank surface and helps conceptualize equivalent control volumes (layers, i.e., *J*) along the tank height. Two thermocouples (T_{in} and T_{out}), each with a 13.5 mm insertion, are installed at the inlet and outlet of the TES, respectively. One thermocouple (T_{tank}) is placed at the outlet of the heating tank. Three others ($T_{sur1,2,3}$) are placed on the tank surface to capture the surface temperature of TES along the tank height. These thermocouples are placed with a uniform axial spacing of 218 mm. Additionally, two more thermocouples ($T_{c.w.in}$ and $T_{c.w.out}$) are located at the terminals of the discharging helical coil, with a 4 mm insertion. Therefore, 16 thermocouples in total are used in the experimental setup. The thermophysical properties of the Hytherm-600 and the materials used in fabricating the tank and the coil are mentioned in previously reported studies [3, 10].

3.2 Operational procedure

The operating conditions considered in the various experimental trials are summarized in **Table 1**. During stand-alone operation, the fully charged TES is kept in standby mode for 6 hours to facilitate thermal stratification in the tank and to demonstrate the reliability of heat retention at the end of the stand-alone period since the stored heat content is prone to losses caused by natural convection. In this pursuit, three experiments with three different charging temperatures have been conducted (**Cases *R1*** to ***R3***). After evaluating heat retention characteristics, the remaining nine experiments are conducted with a 3 h (t = 10800 s) stand-alone period followed by a discharging process, as specified in **Table 1**. The uncertainties have been quantified for the measured and derived quantities. The uncertainties in the derived quantities, i.e., energy stored in the tank and discharging efficiency are estimated using equation (1) [9].

$$\frac{\delta S}{S} = \pm \frac{1}{S} \sqrt{\sum_{i=1}^{m} \left(\frac{\partial S}{\partial X_i} \delta X_i \right)^2} \quad (1)$$

where S is the derived quantity, X is the measured variable, and m denotes the number of variables. The uncertainties associated with the measured temperature, energy stored, discharging energy, and the rate of energy discharged are ±0.5 °C, ±2.8% ±2.54%, and ±2.14%, respectively. The uncertainty associated with the measured water flow rate is about ±0.1%.

Table 1: Operating parameters for the stand-alone operation

Case	Charging temperature (°C)	Operation time (s)		Water flow rate (L/min)
		Retention	Discharging	
R1	50	21600	-	-
R2	70	21600	-	-
R3	90	21600	-	-
A1	50	10800	10800$^+$ to 15800	0.5
A2	50	10800	10800$^+$ to 13770	1.25
A3	50	10800	1000$^+$ to 12300	2
B1	70	10800	10800$^+$ to 15800	0.5
B2	70	10800	10800$^+$ to 14250	1.25
B3	70	10800	10800$^+$ to 13300	2
C1	90	10800	10800$^+$ to 16300	0.5
C2	90	10800	10800$^+$ to 15000	1.25
C3	90	10800	10800$^+$ to 13800	2

3.3 Energy performance

The energy analysis pertinent to the experiments mentioned above energy is conducted as follows:

The amount of thermal energy stored inside the storage tank during one complete cycle of operation can be estimated using equation (2). The stand-alone (or retention) phase begins at the end of the charging process, and a uniform temperature is obtained inside the TES tank.

$$E_{stored} = \rho_o V_{tank} C_{p,o} \left(T_{avg}(t) - T_{ini,\,tank}\right) \quad (2)$$

The amount of energy discharged depends on the difference between water temperatures at the terminal ends of the coil. The discharging process ends once the temperature difference at coil terminals diminishes to 0.5 to 0.7 °C. The rate of energy discharged can be calculated using equation (3).

$$E_{dis} = \dot{m}_w C_{p,w} \left(\bar{T}_{c,\,out}(t) - T_{c,in}\right)\left(t_{q+1} - t_q\right) \quad (3)$$

4. RESULTS AND DISCUSSION

4.1 Retention process

During the three stand-alone experiments of 6 h duration (**Cases *R1- R3***), a degradation of the temperature gradient is observed in the lower portion of the storage tank, primarily due to the losses to ambient and also because a portion of the energy is taken away by the static water residing inside the helical coil as well as the tank wall which has a significant volumetric heat capacity (4031 kJ/m^3. K). On the other hand, nearly a uniform temperature is observed over a large portion of the upper region.

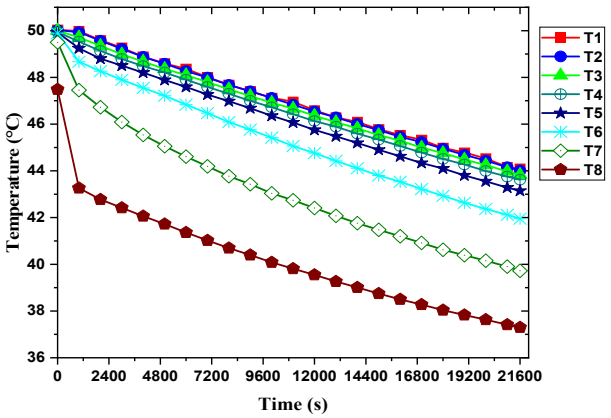

Figure 2: Temporal variation of temperature (Case R1).

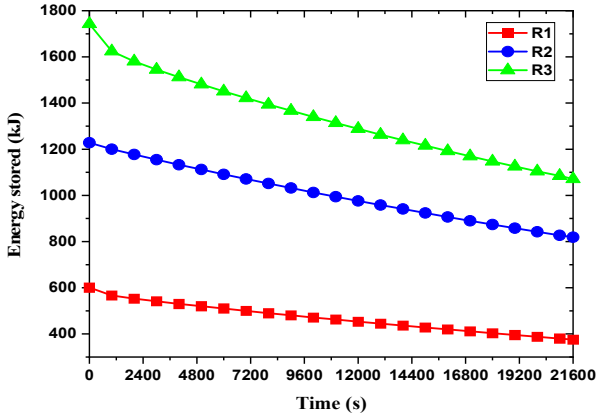

Figure 3: Variation of stored energy over the 6h stand-alone period.

Figure 2 shows the temporal temperature variation within the TES for **Case *R1***. It can be observed that within 3 h (10800 s), a thermocline forms with a hot region extending up to *T6* (81% of tank height measured from the top). It can be noted that *T1* is located 40 mm away from the tank top. The amount of energy stored decreases with time, as shown in **Figure 3**. A higher charging temperature leads to a higher amount of energy stored. However, it also increases the losses to the ambient. The rates of energy losses are 0.01, 0.02, and 0.03 kW for **Cases *R1*, *R2*, and *R3***, respectively.

4.2 Discharging process

A temperature-gradient region with a thickness of 82 mm is found to be formed in the lower portion of the tank at the commencement of the stand-alone operation. **Figure 4** depicts the spatial variation of the temperature along the height of the storage tank for **Case *B1*** at various time instants. The thermocline begins to broaden at t = 3000 s. By the end of the 3h (10800 s) period, the thermocline thickness is approximately 154 mm. Once the discharging process begins, energy is extracted by the water flowing through the helical coil. This causes the splitting of the primary thermocline into two separate regions, and a secondary thermocline is formed below the coil inlet level. The secondary thermocline vanishes due to continuous energy extraction by the helical coil. The primary thermocline residing in the upper region of TES is governed by the thermo-physical properties of the oil.

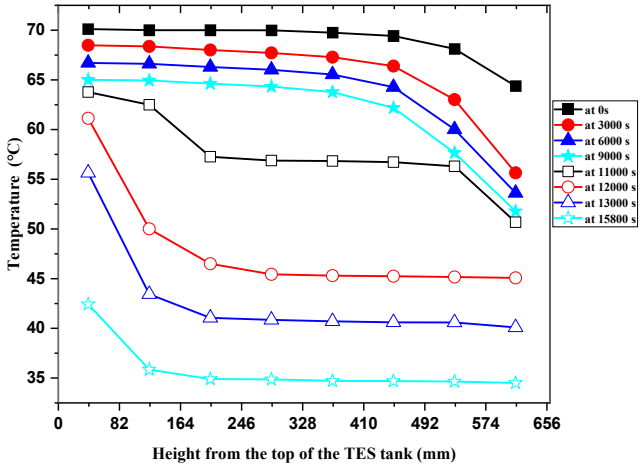

Figure 4: Variation of temperature along the tank height for Case B1 (Starting at a 40 mm distance from the top).

4.3 Energy analysis

Figure 5 shows the variation of energy stored with time for all the cases associated with the discharging operation. At the commencement of the stand-alone operation (t = 0 s), the average energy stored in the TES tank is estimated to be 605 kJ, 1185.5 kJ, and 1751.2 kJ for **Cases *A1– A3*, *B1– B3*,** and ***C1–C3***, respectively.

During the retention period (t = 0 to 10800 s), the stored energy decreases due to convective heat losses to the

environment. The amount of heat extracted during the discharging operation depends on the coil side flow rate.

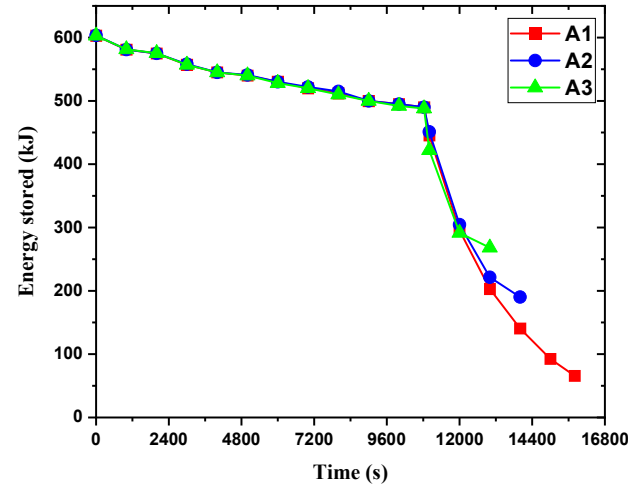

(a) Cases *A1* to *A3*.

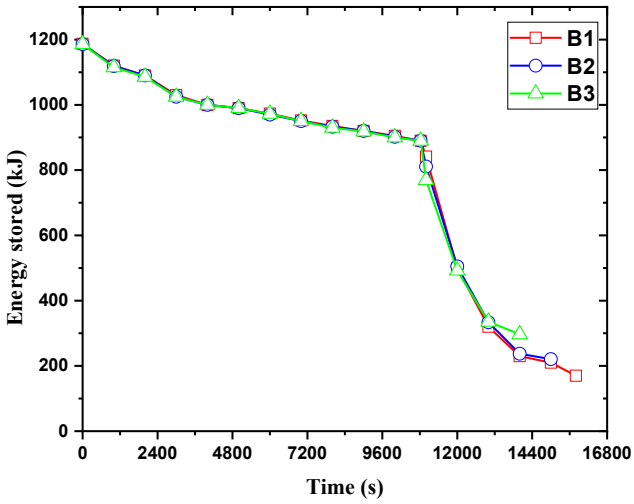

(b) Cases *B1* to *B3*.

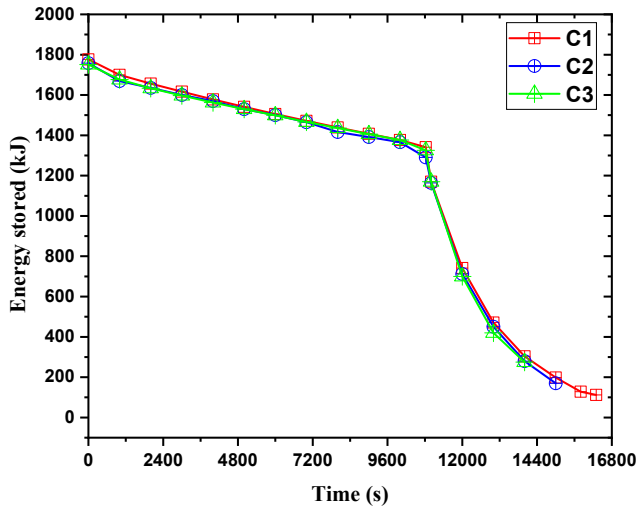

(c) Cases *C1* to *C3*.

Figure 5: Variation of energy stored for all Cases.

It is observed that with a higher water flow rate, the stopping criteria (temperature difference of 0.5 to 0.7 ℃ between coil terminals) is achieved with higher heat content remaining inside the TES. Heat transfer occurs more effectively with a lower water flow rate (0.5 L/min), leading to better energy-harnessing features.

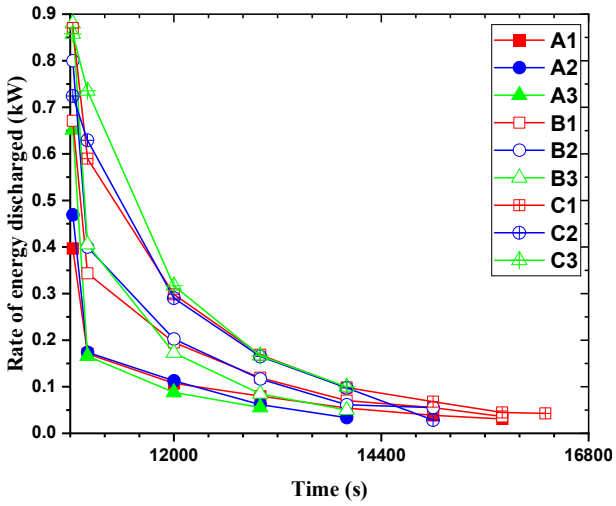

Figure 6: Rate of energy discharged for all Cases.

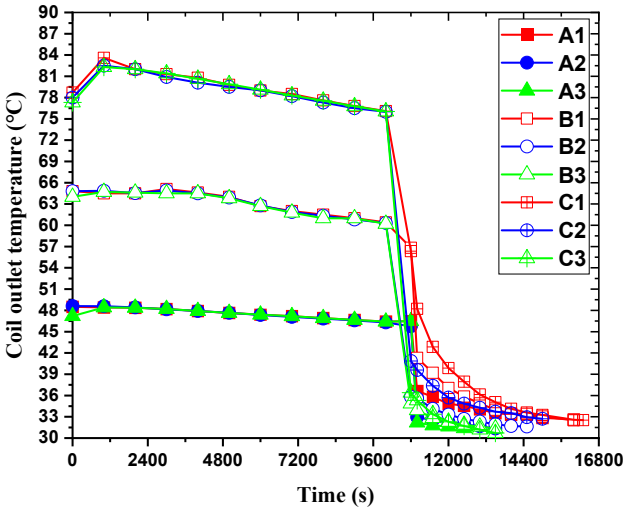

Figure 7: Coil outlet temperature for all Cases.

Figure 6 shows the temporal variation of the rate of energy discharged for the nine cases. At the beginning of the discharging process, the static water inside the helical coil is replaced by fresh cold water. This static water reaches thermal equilibrium with the TES during the stand-alone period by gradually capturing energy from the tank-side oil. Initially, a higher water flow rate offers higher energy transfer. However, as time progresses, the coil outlet temperature drops with increasing water flow rate, reducing energy extraction. **Cases *A1*, *B1*,** and ***C1*** (with coil side flow rate of 0.5 L/min) continue to extract energy from the TES tank over a longer period, owing

to a long residence time of water inside the helical coil. **Figure 7** shows the coil outlet temperature for each case. The average water temperature at the coil inlet is 30 ± 0.5 ℃. However, for the 0.5 L/min discharging flow rate (**Cases *A1*, *B1,* and *C1***), the temperature is 31 ± 0.5 ℃ due to the enthalpy added by the pump. Using the aforesaid stopping criterion, the total operational durations for the different cases are decided, as provided in **Table 1**.

Table 2: Energy analysis for the experimental runs

Case	Energy stored at t = 10800 s (kJ)	Energy discharged (kJ)	Energy losses (kJ)
A1	490.2	420	70.2 (14.3%)
A2	488.9	300.3	188.6 (38.5%)
A3	489.3	183.4	305.9 (62.5%)
B1	896.2	678	218.1 (24.3%)
B2	891.4	631.2	260.2 (29.2%)
B3	890.9	520	370.9 (41.6%)
C1	1330.5	1086.7	243.8 (18.3%)
C2	1325.6	980.8	344.8 (26%)
C3	1341.5	863	478.4 (35.6%)

Table 2 provides an account of the amount of energy stored at the end of the stand-alone period, energy discharged, and losses for each case. Evidently, the cases involving a low water flow rate (0.5 L/min) exhibit a higher amount of energy discharged by the coil. **Figure 8** shows the temperature distribution within the tank-side oil. The representation shows half of the tank with a radial stretch of 81.5 mm. Four different time instants for **Case *C2*** have been presented in **Figures 8a to 8d**, in which the diffusion, stratification, and heat transfer phenomena can be easily noted. **Figure 8 (a)** shows that at t = 3000 s (during the retention period), up to 600 mm of the tank height measured from the top belongs to the hot region (i.e., local temperature ≥ 90% of charging temperature), whereas a thermocline is formed in the lower half of the TES as time progresses. With a higher temperature on the tank side, the temperature gradient between the insulation and ambient increases, leading to increased losses. **Figure 8 (b)** shows a decrease in the oil temperature at the end of the retention process (t = 10800 s). Thermocline thickness is wider (attains a thickness of ~ 154 mm) at this instance, and the hot region stretches to a distance of 500 mm from the tank top. The discharging process begins at t = 10800 s, and as time progresses, the coil side extracts more energy from the tank. During the discharging phase, the convection becomes more dominant compared to the stand-alone period. Therefore, the hot fluid floats to the top of the tank, whereas the colder fluid bulk sinks to the bottom owing to the difference in density, as observed in **Figure 8 (c)**. **Figure 8 (d)** shows the temperature distribution within the oil at the end of the discharging process for **Case *C2*** (t = 15000 s). A uniform temperature is observed in the lower portion of the tank (region between tank heights of 200 mm to 654 mm measured from the top). Once the heat extraction by the coil side fluid weakens due to the reduced temperature difference between the coil terminals, heat diffusion becomes a dominant process, resulting in further degradation in the temperature gradient across the tank height. The de-stratification of the tank is further aggravated by the convection heat transfer to the coil, conduction heat transfer to the storage tank wall, convection heat transfer to the ambient, and continuous heat diffusion towards the tank bottom through the different layers of oil.

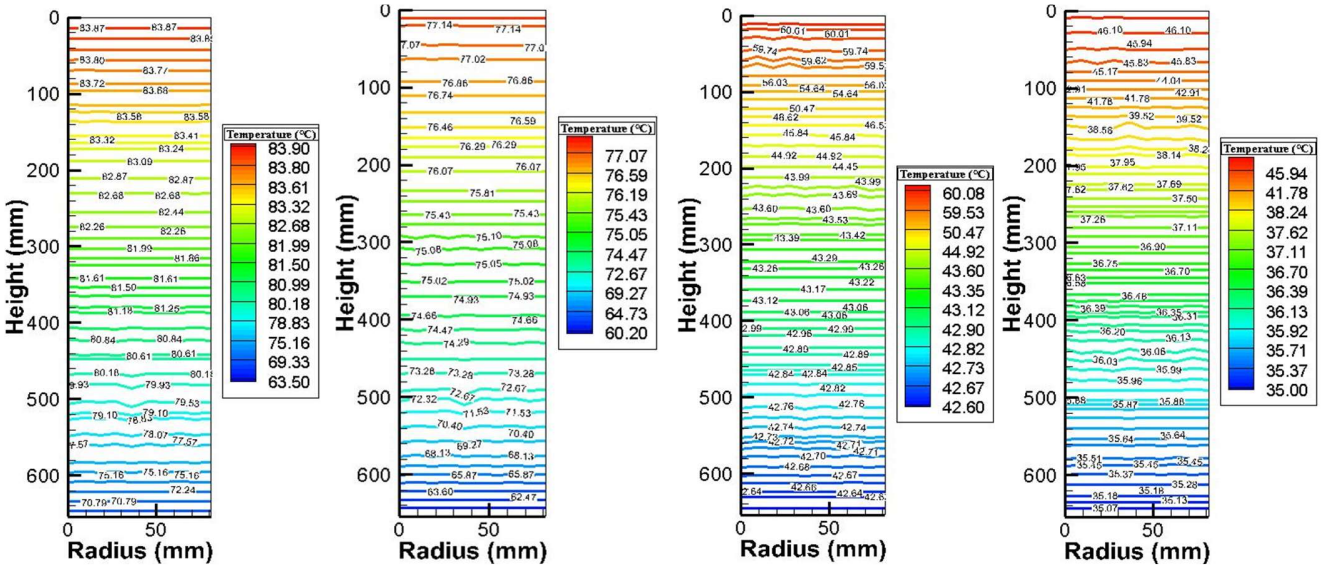

(a) t = 3000 s **(b) t = 10800 s** **(c) t = 13000 s** **(d) t = 15000 s**

Figure 8: Temperature contours (Isotherms) within the Hytherm-600 for Case *C2*.

5. CONCLUSIONS

In this study, Hytherm-600 is used as the energy storage medium in a sensible heat thermal energy storage for demonstrating the heat retention and energy harnessing features. Experimental investigations have been conducted using a vertical cylindrical TES with a helical discharging coil placed inside. The temperature distributions within the tank, the amount of energy stored, the evolution of the thermocline, and the variation in the coil outlet temperature during the discharging operations served as the main performance indicators. The energy analysis for the TES tank has been carried out based on the first law of thermodynamics. It is observed that higher charging temperatures lead to increased losses. The rates of energy losses are 0.01, 0.02, and 0.03 kW for charging temperatures of 50 °C, 70 °C, and 90 °C, respectively. The thermocline thickness broadens as time progresses. It is observed that with a lower water flow rate (0.5 L/min) through the coil, the amount of heat discharged is higher compared to the coil side flow rates of 1.25 L/min and 2 L/min. The thermophysical properties of the Hytherm-600 oil have been found to affect the thermal performance of the storage tank by suppressing the convective heat transfer phenomena. This study also provides insights pertinent to the energy-harnessing features of a storage system using silicone oil and demonstrates the extent of heat retention for different operating conditions. The present study is limited to the maximum operating temperature, which is 220 °C, corresponding to the flash point temperature of Hytherm-600. As an extension of this study, a detailed numerical model needs to be developed for deeper analysis of oil-based TES involving different tank geometries and coil configurations. In addition, a different mode of operation can be analyzed to evaluate the impact of the thermophysical properties of Hytherm-600.

NOMENCLATURE

E	Amount of energy	[kJ]
T	Temperature	(°C)
V	The volume of the tank	(L or m^3)
Cp	Specific heat capacity	[kJ/kg.K]
ρ	Density	[kg/m^3]
$\dot{m}$	Mass flow rate	[kg/s]
t	Time	(s)

REFERENCES

[1] H. Khurana, S. Tiwari, R. Majumdar, and S. K. Saha, Comparative evaluation of circular truncated-cone and paraboloid shapes for thermal energy storage tank based on thermal stratification performance, J Energy Storage, 34, 2021. DOI: 10.1016/j.est.2020.102191

[2] H. Khurana, R. Majumdar, and S. K. Saha, Response Surface Methodology-based prediction model for working fluid temperature during stand-alone operation of vertical cylindrical thermal energy storage tank, Renew Energy, 188, 2022, pp. 619–636. DOI: 10.1016/j.renene.2022.02.040

[3] H. Khurana, R. Majumdar, and S. K. Saha, Experimental investigation of heat dispatch controllability through simultaneous charging-discharging and stand-alone discharging operations in vertical cylindrical sensible heat storage tank, J Energy Storage, 54, 2022. DOI: 10.1016/j.est.2022.105268

[4] H. Khurana, R. Majumdar, and S. K. Saha, Thermal stratification characteristics during simultaneous charging and discharging for different storage tank geometries with the immersed discharging coil, Applied Thermal Engineering, 225, 2023. DOI: 10.1016/j.applthermaleng.2023.120235

[5] H. Khurana, R. Majumdar, and S. K. Saha, Numerical investigation on the performance of the helical and conical coil heat exchanger configurations in the dynamic mode of heat. Proceedings of the 2nd International Conference on Recent Advances in Fluid and Thermal Sciences 2020 (iCRAFT2020), 19–21 March 2021, Dubai, United Arab Emirates. DOI: 10.1063/5.0134122

[6] D. G. Prabhanjan, T. J. Rennie, and G. V. Raghavan, Natural convection heat transfer from helical coiled tubes, International Journal of Thermal Sciences 43, 359–365 (2004).

[7] J. Fernández-Seara, C. Piñeiro-Pontevedra, and J. A. Dopazo, On the performance of a vertical helical coil heat exchanger. Numerical model and experimental validation, Applied Thermal Engineering, 62(2), 2014, pp. 680–689, 2014.

[8] S. Ayuob, M. Mahmood, N. Ahmad, A. Waqas, H. Saeed, and M. B. Sajid, Development and validation of Nusselt number correlations for a helical coil based energy storage integrated with solar water heating system, J Energy Storage, 55, 2022.

[9] A. Kumar, and S. K. Saha. Experimental and Numerical Study of Latent Heat Thermal Energy Storage with High Porosity Metal Matrix under Intermittent Heat Loads. *Applied Energy* 263, 2020, Article 114649. DOI: 10.1016/j.apenergy.2020.114649

[10] R. Majumdar, S. Singh, and S. K. Saha, Quasi-steady state moving boundary reduced order model of two-phase flow for ORC refrigerant in solar-thermal heat exchanger, Renew Energy, 126, 2018, pp. 830–843. DOI: 10.1016/j.renene.2018.04.008